Breaking of general rotational symmetries by multidimensional classical ratchets

A. W. Ghosh[1] and S. V. Khare[2]
[1]*School of Electrical and Computer Engineering, Purdue University, West Lafayette, Indiana 47907*
[2]*Department of Materials Science and Engineering, University of Illinois at Urbana-Champaign, Urbana, Illinois 61801*
(Received 13 December 2002; published 14 May 2003)

We demonstrate that a particle driven by a set of spatially uncorrelated, independent colored noise forces in a bounded, multidimensional potential exhibits rotations that are independent of the initial conditions. We calculate the particle currents in terms of the noise statistics and the potential asymmetries by deriving an *n*-dimensional Fokker-Planck equation in the small correlation time limit. We analyze a variety of flow patterns for various potential structures, generating various combinations of laminar and rotational flows.

DOI: 10.1103/PhysRevE.67.056110 PACS number(s): 05.10.Gg, 05.40.−a, 87.10.+e

I. INTRODUCTION

One of the cornerstones of equilibrium statistical mechanics is the second law of thermodynamics, which precludes extraction of pure work out of a heat source (e.g., a thermal noise) without an accompanying change of state [1]. Fluctuation-dissipation theorem makes it impossible for a system to extract work out of a noise source in equilibrium with it, even if the system is in a potential with a built-in directionality. The impossibility of such a thermal noise-induced rectification was lucidly explained by Feynman [2] using the concept of a ''ratchet,'' a device whose static potential is periodic, but with a spatial asymmetry within each period (such as a sawtooth potential). Although motion in a ratchet is easier in one direction than the other, it is impossible to exploit this asymmetry to drive a particle in the potential using a simple thermal environment. This is because the probability of a noise-induced jump over a barrier in a ratchet depends only on the barrier height, and is therefore the same to the right and to the left, irrespective of the different slopes in the two directions.

Directed motion in a ratchet potential requires an external source of energy that is *out of equilibrium* with the system, thus negating the necessity to obey the fluctuation-dissipation theorem [3,4]. A trivial example is a fully correlated noise source such as a deterministic unidirectional force exerted to an axle attached to a ratchet wheel. Remarkably, the rectification persists even for a nonequilibrium noise force with zero time average. The minimal condition for a ratchet to operate is *broken detailed balance* (such as a ''colored'' or temporally correlated external noise) which in conjunction with the *spatial asymmetry* within each ratchet period, and *broken time-reversal symmetry* (dissipation) leads to directed motion.

The successful extraction of work out of a nonequilibrium source of energy has far-reaching implications. Thermal ratchets are not limited by energetic restrictions associated with equilibrium statistical mechanical principles [4–8]. Massive (underdamped) ratchets exhibit a parametric current reversal that could be useful for continuum mass separation [9,10] and designing ''molecular shuttles'' [11]. Furthermore, ratchet motion is considered to be a possible explanation for the long-range cellular transport of motor proteins [12]. On the experimental front, Brownian ratchets have been demonstrated in the rectified motion of polystyrene spheres and a drop of mercury [13], and in current rectification in a dc superconducting quantum interference device [14].

A ratchet-induced rectification using a two- or three-dimensional apparatus has been investigated recently, primarily with the aim of separating particles of different diffusion constants or sizes [10,15]. Though the particle motion in such studies [10,15,16] is in multidimensions the ratchet effect is usually along a single direction. Relatively little investigation has been done on systems where the ratchet effect exists in multiple spatial directions [17,18]. Extending ratchet motion to higher dimensions involves more than just a simple extension of one-dimensional arguments. One can envisage breaking of higher symmetries such as rotational symmetry, by the broken detailed balance, leading to a rich structure of loops and vortices. Generalizing the concept of a ''coordinate,'' one can map the motion of a stochastic particle in phase space (semiclassical evolution in a multiquantum well system, for example), or in chemical coordinates, into an *n*-dimensional motion in real space. The interplay of rectification and dimensionality can lead to very interesting flow patterns. For instance, a judicious combination of one-dimensional ratchets can lead to steady-state rotations, even if the noise sources themselves are restricted only to apply along the orthogonal directions and are uncorrelated with each other. A simple realization in two dimensions (2D) is as follows: Consider Fig. 1, where a two-dimensional rotation due to ratchet motion is shown schematically. In the presence of spatial asymmetry in one dimension, a time-correlated noise is known to produce a drift [3,21]; the direction of the drift is determined by the sense of the potential asymmetry. For a potential in multiple dimensions, the sense of the potential asymmetry along one coordinate can be reversed by varying the other coordinates, leading to a change in sign (or reversal of asymmetry) of the potential. As indicated in Fig. 1, the coordinate-dependent reversal of the one-dimensional drifts could then conspire together to generate a steady-state rotation. Contrary to rotation generated by purely potential forces, determined by the initial conditions of the particle, the sense of our rotation is *independent* of initial conditions and is given by the combination of the potential asymmetry and the noise statistics. Furthermore, removing either the potential asymmetry or the correlation in the noise destroys the rotation. In effect, we have thus produced a rotational motion

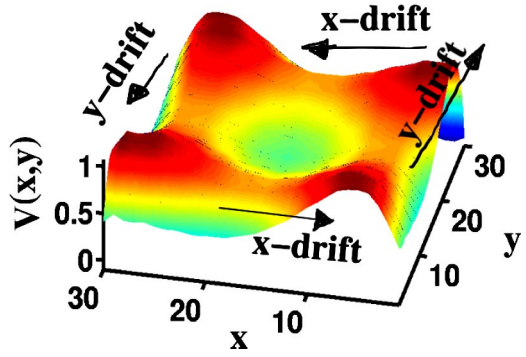

FIG. 1. Schematic description of rotation over one unit cell of a two-dimensional periodic potential, caused by spatial asymmetry and temporal correlations. One-dimensional drifts are produced by asymmetric potentials in x and y, in conjunction with time-correlated noise. The drifts along the x and y directions switch signs owing to coordinate-dependent changes in overall sign of the potential asymmetry, and in combination produce rotation. A specific example of a potential $V(x,y)$ that generates these flows is shown in gray.

along a cyclical track using combinations of one-dimensional ratchets, although the x and y noise forces are totally uncorrelated. A generalization of this process can generate rotations for any asymmetric potential in x and y that is nonseparable in the individual coordinates. Rotation then becomes a necessary outcome of motion in such a potential [18].

In this paper, we develop a formalism for dealing with classical ratchet motion in n dimensions. We generate a bona-fide Fokker-Planck equation (FPE) in terms of a systematic expansion in the correlation time for a Gaussian distributed noise. The work is presented as follows. Section II sets up the functional calculus in arbitrary dimensions that allows us to derive a bona-fide FPE in the presence of colored noise. The formalism in itself is nonperturbative in the noise color. In Sec. III, we derive the n-dimensional FPE. In Sec. IV we specialize to the case of one-dimension and analyze the ratchet motion. We also discuss the various length and time scales built into the dynamical process of a particle in a potential driven by colored noise. In Sec. V, we present a time-dependent solution to the n-dimensional FPE, just before steady state is reached. In Sec. VI, we analyze the steady-state part of the solution of Sec. V and describe the variety of flow patterns that may arise in two and three dimensions. We conclude in Sec. VII. Appendix A gives some algebraic details of the calculations. Appendix B discusses questions about convergence.

II. FUNCTIONAL CALCULUS FOR THE PROBABILITY IN MULTIPLE DIMENSIONS

Consider an overdamped classical particle in a multidimensional potential $U(\vec{r})$ driven by an external time-correlated noise with force $\gamma\vec{f}(t)$, where γ is the damping constant. The motion of the particle is governed by the Langevin equation, which is essentially Newton's law without the inertial term:

$$\dot{\vec{r}}(t)=\vec{W}(\vec{r})+\vec{f}(t), \tag{1}$$

where $\vec{r}(t)$ is the position vector of the particle at time t, $\gamma\vec{W}=-\vec{\nabla}U(\vec{r})$ is the force exerted by the potential on the particle, and the dot over $\vec{r}(t)$ denotes a derivative with respect to time. The stochastic process described above depends crucially on the statistics of the noise $\vec{f}$. We assume that the noise has a Gaussian probability distribution with a correlation time τ_i^c and strength D_i along the ith coordinate direction. Furthermore, we assume that the noise along any two orthogonal coordinate directions are uncorrelated. The probability distribution $P(\vec{r},t)$ [22] can be described in terms of a functional integral over different realizations of $\vec{f}$ as follows:

$$P(\vec{r},t)=\int \vec{\mathcal{D}}fP[\vec{f}]\delta(\vec{r}-\vec{r}(t)),$$

$$P[\vec{f}]=N\exp\left[-\frac{1}{2}\int\int dsds'\sum_{ij}K_{ij}(s-s')f_i(s)f_j(s')\right],$$

$$\langle f_i\rangle=0;\quad \langle f_i(t)f_j(t')\rangle=\frac{D_i}{\tau_i^c}C_i\left(\frac{|t-t'|}{\tau_i^c}\right)\delta_{ij}. \tag{2}$$

The Dirac δ function in Eq. (2) equates the *arbitrary* position variable $\vec{r}$ with the functional form $\vec{r}(t)$ stipulated by Eq. (1). The dimensionless correlation function C_i can, in principle, have multiple time scales built into it. The formalism we develop can be easily generalized to take such extensions into account.

We generalize the functional calculus outlined by Fox [19] to develop a *bona-fide* Fokker-Planck equation for the probability distribution $P(\vec{r},t)$. Using Eqs. (1) and (2), we get

$$\frac{\partial P(\vec{r},t)}{\partial t}=-\int \mathcal{D}\vec{f}P[\vec{f}]\sum_i \dot{r}_i\frac{\partial}{\partial r_i}\delta(\vec{r}-\vec{r}(t))$$

$$=-\sum_i\frac{\partial}{\partial r_i}[W_i(\vec{r}(t))P(\vec{r},t)+Q_i(\vec{r})], \tag{3}$$

where $Q_i(\vec{r})\equiv\int\mathcal{D}\vec{f}P[\vec{f}]\delta(\vec{r}-\vec{r}(t))f_i(t)$. Using results derived in Appendix A, we can write the product $P[\vec{f}]f_i(t)$ as follows:

$$P[\vec{f}]f_i(t)=\sum_l\int dsP[\vec{f}]f_l(s)\delta_{il}\delta(t-s)$$

$$=\sum_l\frac{D_i}{\tau_i^c}\int dsP[\vec{f}]f_l(s)\int ds'K_{il}(s-s')$$

$$\times C_i\left(\frac{t-s'}{\tau_i^c}\right)$$

$$=-\frac{D_i}{\tau_i^c}\int ds'C_i\left(\frac{t-s'}{\tau_i^c}\right)\frac{\delta P[\vec{f}]}{\delta f_i(s')}. \tag{4}$$

Substituting in Eq. (3),

$$\frac{\partial P(\vec{r},t)}{\partial t} = -\vec{\nabla}\cdot(\vec{W}P) - \sum_{ij} \frac{\partial^2 \tilde{Q}_{ij}}{\partial r_i \partial r_j}, \tag{5}$$

where

$$\tilde{Q}_{ij}(t) = \frac{D_i}{\tau_i^c}\int ds' C_i\left(\frac{[t-s']}{\tau_i^c}\right)\int \mathcal{D}\vec{f}P[\vec{f}]\delta(\vec{r}-\vec{r}(t)) \times \frac{\delta r_j(t)}{\delta f_i(s')}. \tag{6}$$

At this stage, we see that in the presence of color, the stochastic process is non-Markovian, which means that the value of P at time t depends on earlier instants of time s' through the kernel $K(t-s')$, or equivalently, through the correlation function C which represents the inverse of K (Appendix A). To evaluate the role of color, we now need to evaluate the functional derivative in Eq. (6). This is best done with the help of the Langevin equation (1) for $\dot{r}_j$,

$$\frac{d}{dt}\left[\frac{\delta r_j(t)}{\delta f_i(s')}\right] = \frac{\delta \dot{r}_j(t)}{\delta f_i(s')} = \frac{\delta}{\delta f_i(s')}[W_j + f_j(t)] = \sum_k M_{jk}\frac{\delta r_k(t)}{\delta f_i(s')} + \delta_{ij}\delta(t-s'), \tag{7}$$

where we define $M_{ij} \equiv \partial W_i(t)/\partial r_j$. The solution to the above equation is

$$\frac{\delta r_j(t)}{\delta f_i(s')} = H(t-s')\,\delta_{ij}\mathbf{T}\left(\exp\left[\int_{s'}^{t} ds M(\vec{r}(s))\right]\right)_{ji}, \tag{8}$$

as can be verified by direct substitution. In the above, $\mathbf{T}$ is the time-ordering operator and $H(x)$ is the Heaviside step function (defined to be unity for positive x and zero otherwise). Substituting this functional derivative in Eq. (5), we manage to reduce the equation for $P(\vec{r},t)$ into the form of a continuity equation:

$$\dot{P} = -\vec{\nabla}\cdot\vec{J},$$

with

$$J_i \equiv W_i P - \frac{\partial}{\partial r_i}[\Theta_i P],$$

$$\Theta_i \equiv \frac{D_i}{\tau_i^c}\int_0^\infty dt' C_i\left(\frac{t'}{\tau_i^c}\right)\mathbf{T}\left(\exp\left[\int_{t-t'}^{t} ds M(\vec{r}(s))\right]\right)_{i,i}. \tag{9}$$

III. GETTING A *BONA FIDE* FOKKER-PLANCK EQUATION

To get the steady-state ($t\to\infty$) limit of the above equation, we expand the integral inside the exponential:

$$\int_{t-t'}^{t} ds M_{ij}(\vec{r}(s)) \approx t' M_{ij}(\vec{r}(t)) - \frac{t'^2}{2}\sum_k \frac{\partial^2 W_j}{\partial r_k \partial r_j}[W_k + f_k] + O(t'^2). \tag{10}$$

The expansion does not introduce any singularities, as discussed in Appendix B. After changing variables $t' \to x = t'/\tau_i^c$, we can now rewrite Θ_i as

$$\Theta_i = D_i\int_0^\infty dx C_i(x)\mathbf{T}\{\exp[x\tau_i^c M - x^2(\tau_i^c)^2 R/2 + O(x^3(\tau_i^c)^3)]\}_{i,i}, \tag{11}$$

where the matrix R has components R_{ij} given by $R_{ij} = \Sigma_k W_k \partial^2 W_i/\partial r_j \partial r_k$. The components of M and R have dimensions of $1/\tau_i^\gamma \approx U_0/\gamma L_i^2$ (U_0 is the maximum height of the potential and L_i is the length scale of variation of the potential in the ith direction, which equals its period for a periodic potential), while x is dimensionless. For small correlation times $\tau_i^c \ll \tau_i^\gamma$ (time scales described in detail in the following section), we can further Taylor expand the exponent to give us the effective diffusion constant Θ_i in terms of the noise statistics defined by $\{\mu_n^i\}$, where $\mu_n^i \equiv \int_0^\infty dx C_i(x)x^n$ is the nth moment of the noise correlation function. For well-behaved functions with rapidly vanishing higher moments, terms like $x^n(\tau_i^c)^n$ can be ignored for small τ_i^c and large n (cf. Appendix B). Then, we can truncate the equation of motion for $P(\vec{r},t)$ to second order, leading thereby to a bona-fide Fokker-Planck equation. For small correlation time τ_i^c, the equation reads

$$\frac{\partial P(\vec{r},t)}{\partial t} = -\sum_i \frac{\partial J_i}{\partial r_i} = -\sum_i \frac{\partial}{\partial r_i}\left(W_i P - \frac{\partial}{\partial r_i}[\Theta_i P]\right),$$

$$\Theta_i = D_i\left[1 + \mu_1^i \tau_i^c M_{ii} - \frac{(\tau_i^c)^2}{2}\mu_2^i (R - M^2)_{ii}\right],$$

$$M_{ij} \equiv \frac{\partial W_i(t)}{\partial r_j},$$

$$R_{ij} \equiv \sum_k W_k \frac{\partial^2 W_i}{\partial r_j \partial r_k}. \tag{12}$$

The above set of equations are the central equations for all our analyses. *The effect of the noise correlation shows up in the effective diffusion constant Θ_i, which picks up a position dependence [23] in a well-defined manner through the potential gradient terms M and R.* The statistics of the noise shows up through the moments $\{\mu_n^i\}$ of the temporal correlation function.

IV. APPLICATION: 1D RATCHET

Having established an approximate though *bona fide* Fokker-Planck equation for *arbitrary* correlation functions

C_i and *arbitrary* dimensions at small correlation times, we now use our results to obtain the dynamics of a classical particle in various kinds of ratchet potentials. As a first step, we calculate the steady-state current density in a one-dimensional periodic potential using our Fokker-Planck formalism for exponential correlation ($\mu_1=1$, $\mu_2=2$). In one dimension, Θ can be written as

$$\Theta = D[1+\tau^c W' - (\tau^c)^2\{WW'' - W'^2\}] \tag{13}$$

to second order in τ^c and where prime denotes a derivative. The expression for Θ to first-order in τ^c is well known in the literature [19]. However, we need to retain the second order corrections in τ^c to get any nontrivial current density out of the noise, as we shall shortly see.

At steady state ($\dot{P}=0$), the Fokker-Planck equation reads

$$\frac{dJ}{dx}=0,$$

$$J = WP - \frac{d}{dx}[\Theta P]. \tag{14}$$

The continuity equation dictates a constant (x-independent) current. Using an integrating factor $\exp(-\phi)$, where $\phi(x) = \int_0^x dy\, W(y)/\Theta(y)$, "0" being an arbitrary point on the x axis, we solve the above first-order ordinary differential equation for P,

$$P(x)\Theta(x)e^{-\phi(x)} = P(0)\Theta(0) - J\int_0^x dy e^{-\phi(y)}. \tag{15}$$

Imposing periodic boundary conditions $P(0)=P(L)$, $\Theta(0)=\Theta(L)$, one then gets the following equation for the drift current J:

$$J = P(0)\Theta(0)[1-e^{-\phi(L)}] \Big/ \int_0^L dx e^{-\phi(x)}. \tag{16}$$

We can solve for $P(0)\Theta(0)$ by normalizing $P(x)$ within a period with a normalization constant N representing the number of particles within a period at steady state. This yields finally

$$J = \frac{N[1-e^{-\phi(L)}]}{\int_0^L dx \frac{e^{\phi(x)}}{\Theta(x)}\left\{\int_0^L dy e^{-\phi(y)} - [1-e^{-\phi(L)}]\int_0^x dy e^{-\phi(y)}\right\}}. \tag{17}$$

For small correlation times τ^c, using the expression for $\Theta(x)$ from Eq. (13), one can expand $\phi(L)$ as follows:

$$\begin{aligned}\phi(L) &= \int_0^L [W(x)/\Theta(x)]dx \\ &\approx \int_0^L dx \frac{W(x)}{D}[1-\tau^c W'(x) + (\tau^c)^2 W(x)W''(x) \\ &\quad + O((\tau^c)^3)].\end{aligned} \tag{18}$$

The first and second terms in the integrand are proportional to exact derivatives (of U and $W^2/2$, respectively), and vanish due to periodic boundary conditions, so that $J\propto(\tau^c)^2$. This allows us to replace $1-\exp[-\phi(L)]$ in Eq. (16) by the small quantity $\phi(L)$. The current density is then given, to leading order in τ^c, by

$$J = (\tau^c)^2 \frac{N\int_0^L dx W^2(x)W''(x)}{\int_0^L dx e^{-U(x)/\gamma D}\int_0^L dx e^{U(x)/\gamma D}}. \tag{19}$$

A nonzero drift current density in a ratchet is generated because the following two quantities do not vanish: (a) correlation time ($\tau^c \neq 0$), which signifies a nonequilibrium noise that breaks detailed balance and (b) potential asymmetry, meaning that there exists no Δx such that $U(x+\Delta x) = -U(x)$. This makes the integral in the numerator of Eq. (19) nonzero although the integrand itself is periodic.

The dynamics of the particle has three time scales built into it.

(a) Correlation time τ^c. This is the time governing the rate of loss of memory in the noise. A convenient way to view the correlation time (as we establish later in this section) is an effective partitioning of the dynamics such that for times less than the correlation time the motion is ballistic, while for times greater than the correlation time the motion is diffusive.

(b) Diffusion time $\tau^D = L^2/D$. L is the typical length scale built into the potential. For a periodic potential, for example, L denotes the period. τ^D describes the time taken to diffuse over one unit length scale L of the potential.

(c) Drift time $\tau^\gamma = \gamma L^2/U_0$. U_0 is the maximum height of the potential, which serves as a typical energy scale in the problem. The drift time describes the amount of time for an overdamped particle to drift from the maximum to the minimum of the potential over a distance $\sim L$, and serves as the time scale for noise-free motion in the system.

Let us calculate J for a 1D periodic asymmetric potential with period L and height U_0, and impose periodic boundary conditions $P(0)=P(L)$. Using Eq. (19) for J, we get the 1D drift current as

$$J = \frac{(\tau^c\tau^D)^2}{(\tau^\gamma)^5} g\left(\frac{\tau^D}{\tau^\gamma}\right), \tag{20}$$

where $g(x)$ is a factor that depends on the geometry of the potential $V(x)$. Figure 2 shows the steady-state current density for a specific example of a periodic potential for varying correlation times τ^c. The current density is positive, tending to drive the particle out of the potential well in the direction where the restoring force $-dU(x)/dx$ is less.

A heuristic argument can illustrate the origin of the directionality of the current. For a correlation function $\langle f(t)f(0)\rangle = (D/\tau^c)C(|t|/\tau^c)$, one can use Langevin's equation (1) to get

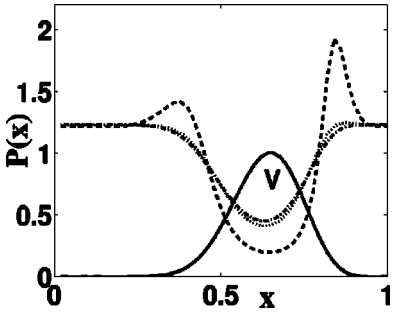

FIG. 2. Potential $U(x)=Ax^{13}(1-x)^7$ (solid line) periodically extended, and the corresponding steady-state probability distributions for $\tau^c=1\times10^{-5}$ (dash-dot), 1×10^{-3} (dotted), and 1×10^{-2} (dashed). Here, the potential height $U_0=1$ and $D=1$. As τ^c increases, the probability peaks to the left in the right well, indicating a positive current density, in the direction of lower restoring force.

$$\langle r^2(t)\rangle = 2Dt\int_0^{t/\tau^c} dY C(Y) - 2D\tau^c\int_0^{t/\tau^c} dY Y C(Y)$$
$$= 2DC(0)t^2/\tau \quad (t\ll\tau^c)$$
$$= 2D[t-\mu_1\tau] \quad (t\gg\tau^c), \tag{21}$$

where μ_1 is the first moment of the noise. The above scaling of the particle coordinate with time means that the particle motion can be looked upon as *ballistic* for $t\ll\tau^c$ and *diffusive* for $t\gg\tau^c$. In absence of correlations ($\tau^c=0$), the particle jumps over the barriers purely due to diffusive transport, and this has equal likelihood in either direction, since the barrier height is the same to the right and to the left. However, for a correlated noise, there is a net drift over an initial time τ^c that pushes the particle ballistically more to the right than to the left, since the restoring force is less to the right (see Fig. 2). At the end of the drift process, therefore, the particle has reached a higher elevation to the right than to the left. Thereafter, the barrier height is smaller to the right, so there is a higher probability of crossing it to the right. Thus, the net drift in the positive x direction is a consequence of *drift assisted thermal activation, produced by the presence of correlation in the noise.*

Figure 2 shows the steady-state probability distribution function for varying values of the correlation time τ^c. For white noise ($\tau^c=0$), the probability distribution is given by the Maxwell-Boltzmann result $P\propto\exp[-U(x)/\gamma D]$. As the correlation time is cranked up, however, the probability distribution within each well of the potential progressively shifts in weight to the left. This corresponds to a nonvanishing steady-state current density J in the positive direction. The direction of the current density can be obtained easily from Eq. (14), whereby the peak ($dP/dx=0$) of the probability density is given for small correlation times ($\Theta\approx D$) by the point where $J=WP$. Since $P>0$, therefore for positive current $J>0$, we have $-W=dU/dx<0$, meaning the peak shifts to the left. Note that the directionality of the ratchet motion depends on the specific nature of the correlation, and can be different depending on whether the time correlation is incorporated into the driving force, or into a fluctuating version of the periodic asymmetric potential we have been dealing with. The current density plotted vs the barrier height shows a maximum, as is seen in Fig. 3. For small barrier heights, there is an equal chance of jumping over the barrier to the right and to the left, so the current is small. Similarly at large barrier heights, the chance is equally small, so the current is small once again. Thus, the peak in the current arises out of a competition between ratchet motion to the right and current backflow to the left.

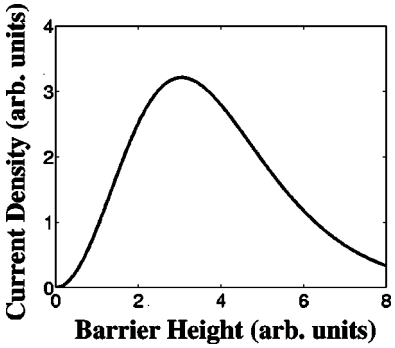

FIG. 3. Steady-state current density for a potential $U(x)=Ax^{13}(1-x)^7$, plotted for varying values of the maximum potential energy U_0. The peak structure arises out of an interplay between increasing ratchet effect and increasing backflow of current as the potential maximum is increased. As U_0 increases from zero, initially the ratchet effect dominates and when it becomes too high the current backflow dominates giving rise to a peak in the ratchet current at intermediate values.

One-dimensional ratchet motion has been observed for polystyrene beads in an aqueous solution driven by a sinusoidal current between lithographically patterned electrodes [13]. In addition, ratchet motion has also been observed for beads in a ''flashing potential'' generated by a laser system modulated suitably by a chopper [3]. In the flashing geometry, the beads are trapped in deep potentials while the laser is on, and allowed to diffuse symmetrically while the laser is turned off. On subsequently turning on the laser, the beads slide back into the wells of the pieces of the potential whose basin of attraction they are individually in. For an asymmetric potential, the beads distribute asymmetrically. The entire process of turning on, switching off, and turning on again leads in effect to a net drift of the particles out of the well in the direction of the steeper slope (*opposite to the drift direction for the noise force-driven ratchet*). Such drifts were reported by direct visual observation.

Our setups can be imagined to be the same, except that the driving force is neither an ac signal nor a switching potential. Instead, we imagine a static asymmetric potential generated as above, but driven by a colored noise generator (the simplest example is a white noise passed through an RC low-pass filter). Imagine a potential with a period ~1 μm ($a=0.7$ μm, $b=0.3$ μm) and fluorescent charged polystyrene beads (~0.07–1 μm) diameter in an aqueous solution at room temperature. The energy of the potential U_0 is set to ≈75 meV. For this set of parameters, $\tau^D\approx3$ s and $\tau^\gamma\approx1$ s. For a piecewise linear potential, $f(\tau^D/\tau^\gamma)\approx\tau^D/\tau^\gamma$. Assume a bandwidth of the colored noise of ~40 Hz (these parameters satisfy $\tau^c\ll\tau^\gamma\ll\tau^D$). Then $\tau\approx10$ h. Such a slow drift of the

fluorescent beads under colored noise should be readily observable with a microscope. Subsequently, measuring the current density for varying values of U_0 should generate a graph similar to Fig. 3, the position of the peak depending on the shape of the potential, but the tail varying as $\exp(-U_0/\gamma D)$.

Let us calculate the efficiency of the ratchet process. Essentially, the energy for the directed motion is extracted from the correlated pieces of the noise force. The input power, given by the product of the force of the noise and the velocity obtained in the absence of the potential, is given by

$$P_{in}=\langle \gamma f \times f\rangle = \frac{\tau^{\gamma}U_0}{\tau^D \tau^c}. \tag{22}$$

To calculate the output power, we use the generated drift velocity and the force $-dU/dx(x)$ required to overcome a potential barrier, and we get

$$P_{out} \approx J \times \frac{U_0}{L}. \tag{23}$$

This yields an efficiency

$$\eta \equiv \frac{P_{out}}{P_{in}} = \frac{(\tau^c)^3(\tau^D)^2}{(\tau^{\gamma})^5}\exp(-\tau^D/\tau^{\gamma}). \tag{24}$$

For the typical values cited above for our proposed experiment, this corresponds to $\eta \approx 10^{-5}$. The transduction is not very efficient, although there have been proposals for ratchet mechanisms that perform almost with 100% Carnot efficiency [20].

V. TIME-DEPENDENT PROBLEM

The steady-state probability distribution obtained in Eq. (12) is, in effect, the long-term ($t\to\infty$) solution to the full time-dependent Langevin problem. To solve for the transient response $P(\vec{r},t)$, let us expand the spatially periodic variables $\vec{W}$ and Θ_i in their Fourier modes: $\vec{W}=\Sigma_{\vec{k}}\vec{W}_{\vec{k}}e^{i\vec{k}\cdot\vec{r}}$ and $\Theta_i=\Sigma_{\vec{k}}\Theta_{i,\vec{k}}e^{i\vec{k}\cdot\vec{r}}$. Expanding $P(\vec{r},t)=\Sigma_{\vec{k}}P_{\vec{k}}e^{i\vec{k}\cdot\vec{r}-i\omega_{\vec{k}}t}$, we get from Eq. (12)

$$\sum_{\vec{k}} -i\omega_{\vec{k}}P_{\vec{k}}e^{i\vec{k}\cdot\vec{r}-i\omega_{\vec{k}}t} = \sum_{\vec{k},\vec{k}'}[-i(\vec{k}+\vec{k}')\cdot\vec{W}_{\vec{k}'} - (\vec{k}+\vec{k}')^2\Theta_{\vec{k}'}]P_{\vec{k}}e^{i(\vec{k}+\vec{k}')\cdot\vec{r}-i\omega_{\vec{k}}t}. \tag{25}$$

Changing summation variables on the right from $\vec{k},\vec{k}'$ to $\vec{k},\vec{k}+\vec{k}'$, we have

$$\sum_{\vec{k}} P_{\vec{k}}e^{-i\omega_{\vec{k}}t}\times\left[i\omega_{\vec{k}}e^{i\vec{k}\cdot\vec{r}} - \sum_{\vec{k}'} i\vec{k}'\cdot\vec{W}_{\vec{k}'-\vec{k}}e^{i\vec{k}'\cdot\vec{r}} - \sum_{\vec{k}'}(k')^2\Theta_{\vec{k}'-\vec{k}}e^{i\vec{k}'\cdot\vec{r}}\right]=0. \tag{26}$$

Setting the terms in square brackets equal to zero, and performing an inverse Fourier transform, we get the dispersion relation

$$-i\omega_{\vec{k}} = -k^2\langle\Theta\rangle - i\vec{k}\cdot\langle\vec{W}\rangle, \tag{27}$$

where $\langle\cdots\rangle$ denotes a spatial average over the period L. Substituting back into the definition of P, and including the steady-state solution as $t\to\infty$, i.e., the long wavelength ($k=0$) limit, we get

$$P(\vec{r},t)=\sum_{\vec{k}\neq 0} P_{\vec{k}}\exp\{i\vec{k}\cdot[\vec{r}-\langle\vec{W}\rangle t]-k^2\langle\Theta\rangle t\}+P_{\rm st}(\vec{r}), \tag{28}$$

as one expects for a drift-diffusion equation. Since the average effective diffusion constant $\langle\Theta\rangle$ is positive, the probability distribution decays with time to the stable steady-state solution.

The "initial conditions" for the Fourier coefficients $P_{\vec{k}}$ in Eq. (28) are set by the value of $P(\vec{r},t_0)$, where $t_0 \gg \tau^c$. We get $P_{\vec{k}}=\int d^3\vec{r}P(\vec{r},t_0)\exp[-\vec{k}\cdot\vec{r}+k^2\langle\Theta\rangle t_0]/L^3$. At times less than τ^c, memory effects become important, the temporal evolution is non-Markovian and the corresponding equation for the probability distribution $P(x,t)$ cannot be truncated to second derivatives in x to construct the bona-fide FPE. This means that for small times the transient equation is not of a drift-diffusion form, but depends in fact on higher correlations. This disallows the use of the FPE structure to start from an initial condition at $t=0$ and propagate to a steady state. However, using an intermediate distribution at t_0 (with $t_0 \gg \tau^c$) is allowed. In order to obtain this intermediate distribution from an initial condition at $t=0$, one actually needs to work with Eq. (9), which has a more complicated time dependence and associated memory effects built into it. However, for times much larger than the lifetime of the memory effects ($\sim\tau^c$), Eq. (28) should work well. For times larger than the correlation time τ^c, the approach to equilibrium is governed by the diffusion constant averaged over a potential period $\langle\Theta\rangle$, while the associated drift is governed by the corresponding average potential force $\langle W\rangle$, which is zero for a periodic potential.

VI. MULTIDIMENSIONAL ANALYSIS: ROTATIONS AND PATTERNS

Let us generalize our results of the previous sections to higher dimensions. We consider a periodic potential so that $U(\vec{r})|_{r_i=0}=U(\vec{r})|_{r_i=L_i}$, where L_i is the period of the potential along the ith direction. Imposing periodic boundary conditions along the ith direction and integrating Eq. 12 leads to an integral equation for J_i,

$$\int_0^{L_i} dr_i J_i(\vec{r})e^{-\phi_i(\vec{r})} = [P(\vec{r})\Theta_i(\vec{r})]|_{r_i=0}[1-e^{-\phi_i(\vec{r})}]_{r_i=L_i}, \tag{29}$$

where

$$\phi_i(\vec{r}) \equiv \int_0^{r_i} dz_i [W_i(\vec{z})/\Theta_i(\vec{z})]. \tag{30}$$

In one dimension, steady-state implies constant current density, which allows us to pull J out of the integrals [as shown in Eq. (15)] and solve for it, with the boundary value of $P(\vec{r})$ at $r_i = 0$ and L_i being fixed by normalization. The situation is quite different in multidimensions. At steady-state, the current density is not a constant, in general. However, we can still make a few observations that lead to nontrivial conclusions: (i) the right-hand side of Eq. (29) is, in general, not identically zero, (ii) the integrand on the left-hand side is a product of $J_i(\vec{r})$ and a positive definite quantity, and (iii) definition of steady state $[\dot{P}(\vec{r},t) \equiv 0]$ implies $\vec{\nabla} \cdot \vec{J}(\vec{r}) \equiv 0$. The first two observations imply that $\vec{J}$ cannot be identically zero everywhere. Combining this with the third observation leads to the unavoidable conclusion that $\vec{\nabla} \times \vec{J}$ is not *identically* zero over one period of the potential (excluding the trivial case where $\vec{J}$ is a constant vector). In other words, there necessarily are local rotational patterns.

The necessity of color and potential asymmetry in our arguments is now easily seen. Analogous to Eq. (18) of the one-dimensional case, for small correlation times τ_i^c, we get

$$\phi_i(L_i) = \int_0^{L_i} dz_i \frac{W_i(\vec{z})}{D_i} \Bigg[1 - \mu_1^i \tau_i^c M_{ii}(\vec{z}) + \frac{(\tau_i^c)^2}{2} [\{\mu_2^i R(\vec{z}) - \mu_2^i M^2(\vec{z})\}_{ii} + 2\{\mu_1^i M_{ii}(\vec{z})\}^2] + O((\tau_i^c)^3) \Bigg]. \tag{31}$$

Terms of zeroth and first order in τ_i^c in Eq. (31) are zero since the integrands in them are proportional to exact derivatives (of U and W_i^2, respectively), and vanish due to periodic boundary conditions. Hence, $\phi_i(L_i) \propto (\tau_i^c)^2$. Thus, from Eq. (31), we see that $\phi_i(L_i) = 0$ either for white noise (i.e., when $\tau_i^c = 0$) or when the potential is symmetric within a single period [i.e., the net integral multiplying $(\tau_i^c)^2$ vanishes]. If either of these conditions holds then our observation (i) is invalidated leaving open the possibility that $J_i(\vec{r}) = 0$ everywhere.

Having established the existence of rotations, we need to solve Eq. (12) numerically in n dimensions with given boundary conditions to get specific flow patterns for $\vec{J}(\vec{r})$. For the purpose of illustrations, we specifically adopt the following simplifications: (a) we concentrate on two dimensions $(i = x,y)$, where Eq. (31) becomes

$$\phi_x(L_x,y) = -\frac{(\tau_x^c)^2}{D_x} \int_0^{L_x} dx W_x(x,y) \Bigg[\frac{\mu_2^x}{2} \left(\frac{\partial W_x}{\partial y} \right)^2 - \left(\frac{3\mu_2^x}{4} - \frac{\mu_1^{x2}}{2} \right) W_x \frac{\partial^2 W_x}{\partial x^2} - \frac{\mu_2^x}{2} W_y \frac{\partial^2 W_x}{\partial x \partial y} \Bigg]; \tag{32}$$

(b) next we will consider the specific case of exponential correlation function $(\mu_1^i = 1,\ \mu_2^i = 2)$; (c) finally, we consider a restricted class of potentials and noise such that $U(x,y) = U(y,x)$, $D_x = D_y$, and $\tau_x^c = \tau_y^c$. At steady state, this implies that $J_x(x,y) = J_x(y)$ and $J_y(x,y) = J_y(x)$, i.e., the x component of vector $\vec{J}(x,y)$ is only a function of y and its y component is only a function of x. Before proceeding further, we emphasize that our arguments [following Eq. (29)] showing the necessary existence of rotations do not depend on this restricted class of noises and potentials; the class of potentials is adopted just to simplify the algebra for illustrative purposes. The calculation of $J_x(y)$ and $J_y(x)$ can now proceed smoothly by observing that J_x (or J_y) may be pulled out of the integral in Eq. (29). The total current density $\vec{J}(\vec{r})$ is then obtained by solving the set of Eqs. (29)–(32). The current density $J_x(y)$ depends on the Dirichlet boundary conditions $P(0,y)$, which we will set to a constant $[P(0,y) = P(x,0) = \text{const}]$, since it allows us to get simple flow patterns.

TABLE I. Table showing the general flow patterns that can be constructed by combining appropriate ratchet potentials in multiple dimensions. Examples of such flows are depicted in Figs. 4–7.

Flow pattern	Coupling mechanism
Rotation	Ratchets coupled in x and y
Laminar flow	Decoupled ratchets in x and y
Rotation + net drift	Coupled ratchets asymmetric under $x \leftrightarrow -x$, $y \leftrightarrow -y$

Table I shows the three general cases of multidimensional flows which may be created by appropriate choice of the potential. Figures 4–7 show contour plots of different potentials and their corresponding current densities $\vec{J}$. The first case is shown in Fig. 4 which shows that for nonseparable

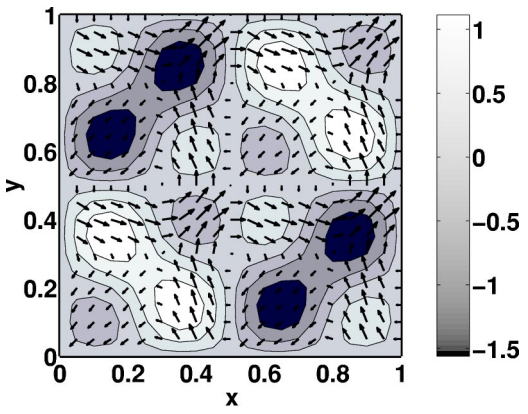

FIG. 4. Contour plots of the potential $U(x,y) = \sin(x)\sin(y) - a\sin(2x)\sin(2y)$ with $a = 1$, and all lengths expressed in units of 2π. White (dark) regions show maxima(minima) of $U(x,y)$. Superposed on top are arrows showing the two-dimensional vector field $\vec{J}(x,y)$, where the arrow lengths are scaled to $|\vec{J}|$. The rotations are produced by inversion of drift currents produced by opposing ratchet potentials in a given direction. The current density $\vec{J}$ scales with the asymmetry parameter "a" and the square of the correlation time τ^c, so for white noise or symmetric potentials, there are no rotations.

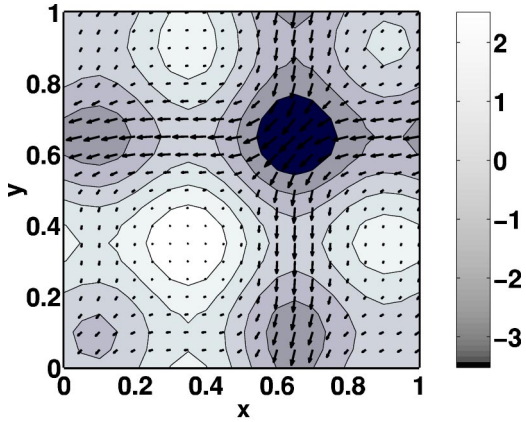

FIG. 5. Same as Fig. 4 with the potential replaced with a separable one $U(x,y)=\sin(x)-\sin(2x)+\sin(y)-\sin(2y)$, which leads to laminar flow, caused by two independent decoupled ratchets in the x and y directions.

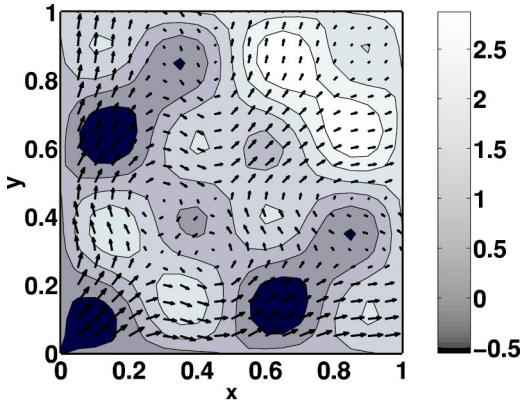

FIG. 6. Combination of drift and laminar flow in coupled potential $U(x,y)=[\sin(x)\sin(y)-\sin(2x)\sin(2y)]+0.2(x+y)$. The term $x+y$ is periodically repeated outside the interval $[0,1]$.

potentials one gets, in general, rotational vortices. This demonstrates the breaking of rotational symmetry of the system by construction of an appropriate ratchet potential. Notice that the total circulation along the boundary is zero, which means that although there are local circulation patterns, the global average is zero. This is a consequence of periodic boundary conditions that we use. Global rotations will need a net rotation along the boundary, which is a different set of boundary conditions (similar to that in Fig. 1) than we are analyzing here. The absence of any global circulation causes the current circulation patterns to come in vortex-antivortex pairs.

Figure 5 shows how in a separable potential one gets a laminar flow. By adjusting the relative magnitude of the potential terms involving the x and y coordinates one can change the angle the laminar flow makes with the x axis. Thus, we can obtain the breaking of reflection symmetry about the two axes x and y, with this flow pattern. Notice that

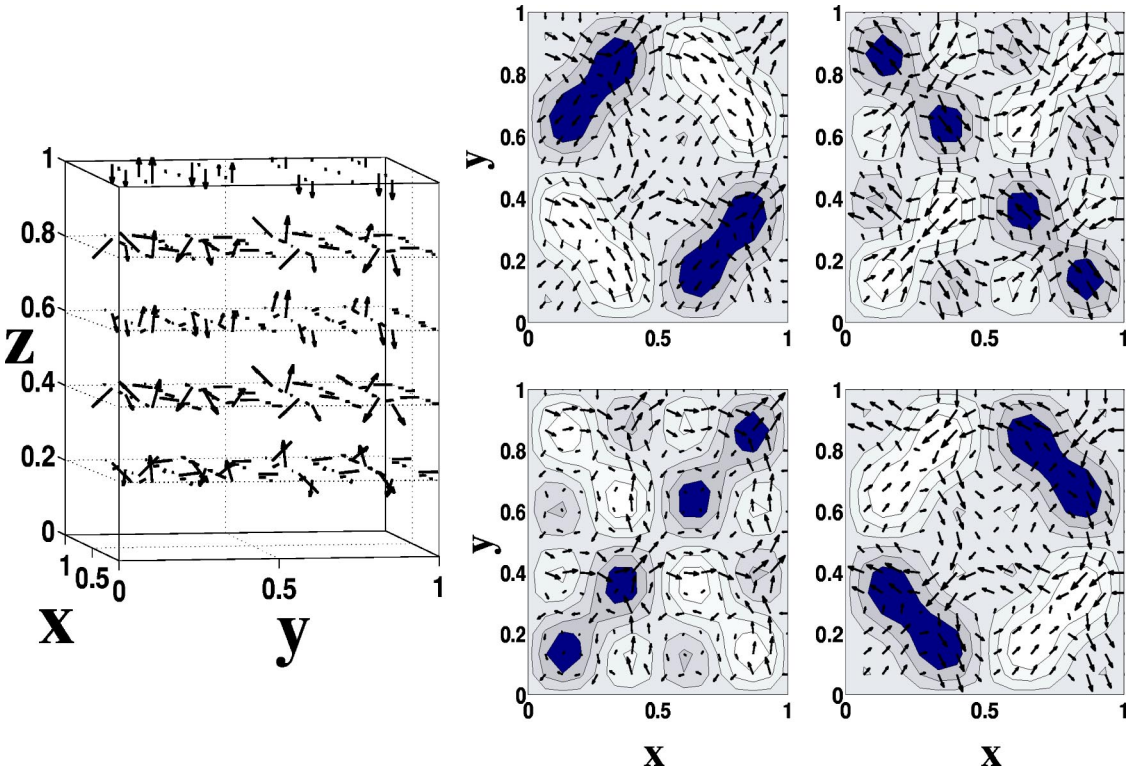

FIG. 7. The 3D flow patterns in the potential $U(x,y,z)=A[\sin x \sin y \sin z-\alpha \sin(2x)\sin(2y)\sin(2z)]$ for $A=1$, $\alpha=1$. The 3D potential leads to a rich structure of loops and vortices (left). In the panels to the right, components J_x and J_y of the current are plotted at various z slices, corresponding to heights $z/2\pi=$ (a) 0.2 (top left), (b) 0.4 (top right), (c) 0.6 (bottom left), and (d) 0.8 (bottom right). Note that the sizes of the arrows show the relative magnitudes of the J_x, J_y currents within each panel, and should not be compared for varying heights (such a comparison is shown in the 3D plot on the left).

although there are local swings in the current density, there are no vortex-antivortex pairs, since only the relative magnitudes (but not the signs) of $J_x(y)$ and $J_y(x)$ change. For a combination of separable and nonseparable potentials as shown in Fig. 6, one gets equivalent combinations of patterns, i.e., one can generate net drifts along with local rotations.

It is a straightforward generalization to produce flow patterns for a three dimensional (3D) potential using approximations similar to those made for Figs. 4–6. Figure 7 shows a flow pattern for a 3D potential, shown as a 3D plot, and as 2D plots at different z slices. Infinitely many combinations of such potentials can be generated to break different kinds of symmetries in higher dimensions as shown in Figs. 4–7. As an example, in 3D one could have a 1D ratchet along the z direction completely decoupled from a rotating 2D ratchet in the x-y plane. This would give rise to a helix with its axis along the z direction.

Finally, we note that we have used Dirichlet boundary conditions with specified $P(x,0)$ and $P(0,y)$ functions (assumed to be constant), in order to get our flow patterns. We could use Neumann boundary conditions as well, by rewriting $P(0,y)$ in $J_x(y)$ in terms of the normal derivative $\partial P(x,y)/\partial x|_{x=0}$. This is done using the definition of $\vec{J}$ from Eq. (9) and in Eq. (29), setting $r_i = x$

$$P(0,y) = \frac{1}{\chi(y)} \Theta_x(0,y) \left. \frac{\partial P(x,y)}{\partial x} \right|_{x=0}, \tag{33}$$

where

$$\chi(y) = \left(W_x(x,y) - \frac{\partial \Theta_x(x,y)}{\partial x} \right)_{x=0} - \Theta_x(0,y) \frac{[1 - e^{-\phi_x(L_x,y)}]}{\int_0^{L_x} dx e^{-\phi_x(x,y)}}, \tag{34}$$

and an analogous equation for $P(x,0)$ in terms of $\partial P(x,y)/\partial y|_{y=0}$.

VII. CONCLUSIONS

We have shown that a Fokker-Planck equation may be derived for a weak colored noise for a bounded potential in multiple dimensions. Using this we have demonstrated that an asymmetric periodic potential with a colored noise in n dimensions will *necessarily* lead to breaking of many types of symmetries of the particle motion. Specific examples have been solved for laminar flow and laminar flow combined with rotations in two and three dimensions. Such symmetry breaking in higher dimensions should also be readily generalizable to other types of noise statistics, such as a non-Gaussian probability distribution, and other types of ratchet potentials. This could include time-dependent (''flashing'') ratchet potentials [25], as well as discrete versions such as multidimensional Parrondo's games [26].

ACKNOWLEDGMENTS

We would like to thank O. Pierre-Louis for suggesting the problem, and C. Jayaprakash, F. Jülicher, J. W. Wilkins, S. Datta, D. Basu, and S. S. Khare for useful discussions.

APPENDIX A: MATHEMATICAL DETAILS

(i) Lemma: $\delta N/\delta f_k(t) = 0$.
Proof.

$$\frac{\delta N}{\delta f_k(t)} = -N^2 \frac{\delta(1/N)}{\delta f_k(t)}. \tag{A1}$$

From the normalization condition $\int P[\vec{f}]\vec{\mathcal{D}}f = 1$ and Eq. (2), we get

$$\frac{1}{N} = \int \vec{\mathcal{D}}f \exp\left[-\frac{1}{2} \int \int ds ds' \sum_{ij} K_{ij}(s-s') f_i(s) f_j(s') \right]. \tag{A2}$$

Hence, we get

$$\begin{aligned} \frac{\delta N}{\delta f_k(t)} &= -N^2 \int \mathcal{D}\vec{f} \exp(\cdots) \left[-\frac{1}{2} \int \int ds ds' \right. \\ &\quad \times \sum_{ij} K_{ij}(s-s') \{ \delta_{ik} \delta(t-s) f_j(s') \\ &\quad \left. + \delta_{jk} \delta(t-s') f_i(s) \} \right] \\ &= N^2 \int \mathcal{D}\vec{f} \exp(\cdots) \sum_i \int ds [f_i(s)/2] \\ &\quad \times [K_{ki}(t-s) + K_{ik}(s-t)] \\ &= (N/2) \sum_i \int ds [K_{ki}(t-s) \\ &\quad + K_{ik}(s-t)] \int \mathcal{D}\vec{f} P[\vec{f}] f_i(s), \end{aligned} \tag{A3}$$

where the second integral on the last line can be rewritten as $\langle f_i \rangle$, which is zero since we assume that the noise has zero average [cf. Eq. (2)]. This completes the proof.

As a corollary to the above, we obtain the following two equations:

$$\frac{\delta P[\vec{f}]}{\delta f_k(t)} = -\sum_i \int ds K_{ik}(t-s) f_i(s) P[\vec{f}], \tag{A4}$$

$$\begin{aligned} \frac{\delta^2 P[\vec{f}]}{\delta f_k(t) \delta f_l(t')} &= -K_{kl}(t-t') P[\vec{f}] \\ &\quad + \sum_{ij} \int \int ds ds' K_{ik}(t-s) \\ &\quad \times f_i(s) K_{jl}(t'-s') f_j(s') P[\vec{f}]. \end{aligned} \tag{A5}$$

(ii) Lemma: $\int ds' K_{il}(t'-s')C_i([s-s']/\tau_i^c)=\tau_i^c\delta_{il}\delta(t-s')/D_i=\int ds' K_{il}(s-s')C_i([t'-s']/\tau_i^c)$.

This equation establishes that K is a diagonal matrix, whose inverse gives C. Differentiating the normalization equation $1=\int \mathcal{D}\vec{f}P[\vec{f}]$, we get

$$0=\frac{\delta^2}{\delta f_k(t)\,\delta f_l(t')}\int \mathcal{D}\vec{f}P[\vec{f}]=\int \mathcal{D}\vec{f}\frac{\delta^2 P[\vec{f}]}{\delta f_k(t)\,\delta f_l(t')}$$
$$=\sum_{ij}\int\int dsds'[K_{ik}(t-s)K_{jl}(t'-s')\langle f_i(s)f_j(s')\rangle - K_{kl}(t-t')]. \quad \text{(A6)}$$

Rewriting $K_{kl}(t-t')$ as $\Sigma_i\int ds K_{ik}(t-s)\delta_{il}\delta(s-t')$, and using $\langle f_i(s)f_j(s')\rangle=\delta_{ij}(D_i/\tau_i^c)C_i([s-s']/\tau_i^c)$ leads immediately to the above proof.

APPENDIX B: CONVERGENCE ISSUES

It is important to establish the validity of various expansions that we do in the correlation time at various stages of the derivation of Eq. (12). In particular, the current distribution may not necessarily be an analytic function of τ^c for an arbitrary noise source, in which case any perturbative expansion in τ^c yields results that are wrong. The nonanalyticity can arise from three possible sources: (i) the potential itself may be nonanalytic, (ii) the noise statistics has a finite support, (iii) the perturbative expansion may be a nonanalytic function of τ^c.

Case (i). A piecewise linear sawtooth potential has infinite derivatives at the kinks, leading to potential divergent terms in the current. This can be avoided, in principle, by restricting our arguments to a smoothened function.

Case (ii). The derivation of the Fokker-Planck structure itself depends crucially on the statistics of the noise. If the noise distribution has a finite support so that arbitrarily large noise amplitudes are excluded from consideration, then any computation of the current density along the lines we prescribed would be totally wrong. For example, if the height of the potential barrier is larger than the maximum allowed noise amplitude, then there will be no current, contrary to what an injudicious application of the formalism will yield. In our analyses, we have assumed a Gaussian distribution function for the noise [Eq. (2)]. This has an infinite support and thereby avoids such nonanalyticities [24]. However, for a discrete noise process such as dichotomous noise, care must be exercised in obtaining the Fokker-Planck description. Often, an additional white noise source is included with the explicit purpose of handling such nonanalyticities. We do not need such sources since our probability distribution is Gaussian.

Case (iii). The functional calculus as outlined by Fox and extended by us to several dimensions is nonperturbative in the correlation time. As argued by Fox in Ref. [19], the prescription leads to currents that are uniformly convergent for $\tau^c=0$. The nonperturbative description leads us to Eq. (9) that involves the exponential of integrals of matrix elements of M. We finally performed an explicit evaluation of the matrix elements in Eq. (11) for small τ^c. This does involve a perturbative expansion in τ^c, but of an exponential function, analytic in τ^c. The nth term of the expansion is proportional to $\mu_n(\tau^c/\tau^\gamma)^n/n!$. For well-behaved correlation functions such as an exponential or a Gaussian, this term tends to zero rapidly as n increases to infinity, provided $\tau^c<\tau^\gamma$, as we have assumed.

[1] K. Huang, *Statistical Mechanics* (Wiley, New York, 1963).

[2] R.P. Feynman, R.B. Leighton, and M. Sands, *The Feynman Lectures on Physics* (Addison Wesley, Reading, MA, 1963), Vol. 1, Chap. 46.

[3] For an overview and references, see P. Reimann, Phys. Rep. **361**, 57 (2002); D. Astumian and P. Hänggi, Phys. Today **55**(11), 33 (2002).

[4] F. Jülicher and J. Prost, Phys. Rev. Lett. **75**, 2618 (1995).

[5] F. Jülicher, A. Ajdari, and J. Prost, Rev. Mod. Phys. **69**, 1269 (1997); A.B. Kolomeisky and B. Widom, J. Stat. Phys. **93**, 633 (1998); M.E. Fisher and A.B. Kolomeisky, Proc. Natl. Acad. Sci. U.S.A. **98**, 7748 (2001).

[6] J. Maddox, Nature (London) **365**, 203 (1993).

[7] M.O. Magnasco, in *Fluctuations and Order: The New Synthesis*, edited by M. Millonas (Springer-Verlag, Berlin, 1994).

[8] R.D. Astumian and M. Bier, Biophys. J. **70**, 637 (1990); C.S. Peskin, G.B. Ermentrout, and G.F. Oster, in *Cell Mechanics and Cellular Engineering*, edited by V.C. Mov, F. Guilak, R. Tran-Son-Tay, and R.M. Hochmuth (Springer, New York, 1994).

[9] I. Derényi and T. Vicsek, Proc. Natl. Acad. Sci. U.S.A. **93**, 6775 (1996).

[10] A. van Oudenaarden and S.G. Boxer, Science (Washington, DC, U.S.) **285**, 1046 (1999); I. Derényi and R.D. Astumian, Phys. Rev. E **58**, 7781 (1998).

[11] F. Marchesoni, Phys. Lett. A **237**, 126 (1998).

[12] I. Derenyi and T. Wicsek, Physica A **249**, 397 (1998).

[13] J. Rousselet *et al.*, Nature (London) **370**, 446 (1994); L.P. Faucheux *et al.*, Phys. Rev. Lett. **74**, 1504 (1995).

[14] I. Zapata, R. Bartussek, F. Sols, and P. Hänggi, Phys. Rev. Lett. **77**, 2292 (1996).

[15] G.W. Slater, H.L. Guo, and G.I. Nixon, Phys. Rev. Lett. **78**, 1170 (1997); D. Ertas, *ibid.* **80**, 1548 (1998); T.A.J. Duke and R.H. Austin, *ibid.* **80**, 1552 (1998); J.F. Wambaugh, C. Reichhardt, C.J. Olson, F. Marchesoni, and F. Nori, *ibid.* **83**, 5106 (1999); A. Lorke, S. Wimmer, B. Jager, J.P. Kotthaus, W. Wegscheider, and M. Bichler, Physica B **249**, 312 (1998); C. Keller, F. Marquardt, and C. Bruder, Phys. Rev. E **65**, 041927 (2002); C.S. Lee, B. Janko, I. Derényi, and A.L. Barabasi, Nature (London) **400**, 337 (1999).

[16] J.K. Gimzewski, C. Joachim, R.R. Schlittler, V. Langlais, H. Tang, and I. Johannsen, Science (Washington, DC, U.S.) **281**, 531 (1998); T.R. Kelly, H. DeSilva, and R.A. Silva, Nature (London) **401**, 150 (1999).

[17] H. Qian, Phys. Rev. Lett. **81**, 3063 (1998).
[18] A.W. Ghosh and S.V. Khare, Phys. Rev. Lett. **84**, 5243 (2000).
[19] R.F. Fox, Phys. Rev. A **33**, 467 (1986); **34**, 4525 (1986).
[20] I.M. Sokolov, e-print cond-mat/0002251.
[21] M.O. Magnasco, Phys. Rev. Lett. **71**, 1477 (1993).
[22] As an alternative the calculation of the probability distribution $P[\vec{f}]$ as in Eq. (2), one could write a dynamic equation for $\vec{f}(t)$ having the form: $d\vec{f}/dt = -\mathbf{A}\vec{f} + \mathbf{B}\vec{\zeta}(t)$, where $\vec{\zeta}$ (t) is a white noise. The solution $\vec{f}$ (t) represents a diffusion process, although it is singular in terms of the diffusion tensor. The rigorous mathematics for the singular diffusion has been recently studied by J.-P. Eckmann and M. Hairer, Commun. Math. Phys. **219**, 523 (2001).
[23] A. Ghosh, Phys. Lett. A **187**, 54 (1994).
[24] H. Kohler and A. Mielke, J. Phys. A **31**, 1929 (1998).
[25] A. Ajdari and J. Prost, C. R. Acad. Sci. Paris **315**, 1635 (1992).
[26] G.P. Harmer, D. Abbot, P.G. Taylor, and J.M.R. Parrondo, Chaos **11**, 705 (2001).